Absolute Positioning Instruments for Odometry System Integrated with Gyroscope by Using IKF

Surachai Panich[1] Nitin Afzulpurkar[2]

GJRE Classification (FOR)
GJRE:F , 671401 099902

Abstract- **In this paper, absolute positioning instrument using trilateration ultrasonic sensor is mainly proposed to estimate absolute position errors combined with estimated position and orientation from differential odometry integrated with gyroscope to calculate absolute position of mobile robot. In the method, the indirect Kalman filter is mainly used to estimate absolute position errors and the estimated errors are fed back to odometry system, and also estimates some parameter errors to correct encoder and gyroscope error. The simulation and experiment results show the estimated position and orientation of odometry system integrated with gyroscope, systematic errors of encoder and gyroscope and absolute position from trilateration ultrasonic sensor compared with odometry system integrated with gyroscope.**

Keywords- absolute positioning, indirect Kalman filter, odometry system, trilateration ultrasonic sensor.

I. Introduction

Typically, mobile robots behavior such as navigation, map building, the estimation of own position is very important. There are a lot of researches regarding the mobile robot in navigation such as (Maeyama, 1996; Borenstein, 1996; Hakyoung, 2001; Bostani, A., et al., 2008; Byoung-Suk Choi, 2009; Takeshi Sasaki, 2010). In navigation system can be categorized in relative and absolute positioning systems. The relative positioning system estimates a current position by using the information about previous positions and velocities. Basically, the method of estimation for a wheel type mobile robot's position uses the wheel encoder called odometry system. This is based on the wheel sensor readings of a differential-drive robot. In odometry (wheel sensors only) and dead reckoning (also heading sensors) the position update is based on sensors information. The movement of the robot sensed with wheel encoders or heading sensors or both, is integrated to compute position. Thus the position has to be updated from time to time by other localization mechanisms. Because the sensor measurement errors are integrated, the position error accumulates over time. However, these cumulative errors can be reduced by additional sensors. In outdoor environment, the estimated position by encoder has the unpredictable error caused by traveling over an unexpected small obstacle or a bump under the wheels. In this case, the accuracy of the estimated robot's position is suddenly getting worse.

About-[1] School of Engineering and Technology, Asian Institute of Technology, P.O. Box 4, Klong Luang, Pathumthani 12120, Thailand, (surachai.panich@ait.ac.th)
About-[2] School of Engineering and Technology, Asian Institute of Technology, P.O. Box 4, Klong Luang, Pathumthani 12120, Thailand, (nitin@ait.ac.th)

The position error is detailed in differential equation either inertia measurement unit (IMU) or support sensors nowadays with some solutions in textbook (Britting, 1971). The analysis of navigation process from Kelly (Kelly, 2001) is under special consideration about systematic error and theory on navigation. Also the compensation of position's error with redundant sensors is discussed (Larsen, 1998; Chung, 2001), however always limits on some redundant support systems. Despite these limitations, most researchers agree that encoder is an important part of a robot navigation system and that navigation tasks will be simplified if encoder accuracy can be improved. For example, the map-based positioning system is the method in absolute positioning system by using environment as landmark (Luis M. Valentin-Coronado, et al., 2009; Sotirios Ch. Diamantas and Richard M. Crowder, 2009). A mobile robot builds a local map by using onboard sensors and compares the local map with a global map. If the features from local map and the global map match, an absolute position of the mobile robot is computed. Researches on the map-based positioning have been mainly focused on creating an accurate local map and estimating the positions by a map matching techniques. Cameras are the most complex sensors recently utilized due to high computational and memory requirements, as well as high cost in robotics. On researches in robotic field are using either local or global vision. In global vision, the camera is used as external instrument to monitor area, which covers both of the robot and environment. The global vision is easy to realize and widely used such as in factory environments or in robotic filed, i.e. the popular competition of robot soccer. The absolute positioning system estimates a current position measuring the position from predefined positions. The position errors of the absolute positioning system are bounded, because the information on previous positions is not required. However the absolute positioning system cannot provide absolute position information along path because of absolute positioning instrument's cost and operation in large area. Therefore, a hybrid navigation system plays an important role in combination of the relative or absolute positioning system by selection one from each category. Optimal localization should take into account the information provided by all of these sensors. A powerful technique for achieving this sensor fusion, called the Kalman filter (Kang Li, et al., 2009). It is a mathematical mechanism for producing an optimal estimate of the system state based on the knowledge of the system and the measuring device, the description of the system noise and measurement errors and the uncertainty in the dynamics models. Thus the Kalman filter fuses sensor information and system knowledge in an optimal solution. Optimality depends on the criteria chosen to evaluate the performance. Within the Kalman filter theory the system is assumed to be linear with Gaussian noise. This paper proposes two main points. The first point is the integration of absolute positioning instruments in navigation process, which can support mainly differential odometry system. For the second point the navigation parameter with complementary support system based on indirect Kalman filter (IKF) and with model of redundant error sources can compensate each other. The indirect Kalman filter can estimates the errors in the navigation and attitude information using the difference between inertial navigation system (INS) and external source data (Maybeck, 1979). The error model is separated between systematic and non-systematic. The different measurement of error level is performed by complement of redundant support system. For all relevant navigation parameters is with concept of relative and absolute support system in form of external redundant source. In scope of hybrid approach the differential odometry and support system for our purpose are combined that the navigation problem in real-time can be solved. By the experimental test sensor information are from real physical sensors. Section 2 describes the generally differential drive for mobile robot including encoder model. Section 3 explains the widely relative support of gyroscope. The trilateration ultrasonic sensor is explained in section 4. The hybrid navigation system is described in section 5. Simulations and experiments are presented in section 6 and finally concludes the paper.

II. DIFFERENTIAL DRIVE FOR MOBILE ROBOT AS MAIN SYSTEM

Generally, in navigation of mobile robot localization plays an important role. The robot‘s position is defined as $\mathbf{P}_k = [\mathbf{X}_k,\ \mathbf{Y}_k,\ \boldsymbol{\theta}_k]^T$ and the next position $\mathbf{P}_{k+1}$ is calculated from current position plus the position‘s increment both translation $\Delta\mathbf{S}_k = [\Delta\mathbf{S}_{x,k}\ \ \Delta\mathbf{S}_{y,k}]^T$ and rotation increment $\Delta\boldsymbol{\theta}_k$ with reference to geometry as

$$\mathbf{P}_{k+1} = \mathbf{P}_k + \begin{bmatrix} \Delta\mathbf{S}_{x,k} \\ \Delta\mathbf{S}_{y,k} \\ \Delta\boldsymbol{\theta}_k \end{bmatrix} \qquad (1)$$

With the increment $\Delta\mathbf{S}_k$ and $\Delta\boldsymbol{\theta}_k$ are used as couple function to construct mobile robot. In the differential drive system may consider that mobile robot move in curve path. Generally, the kinematics of differential drive consists of two wheels with wheel base $\mathbf{B}_k$. In Fig.1 mobile robots are widely integrated with encoders at the left and right wheels, which generate the increment translation $\Delta\mathbf{S}_{L,k}$ and $\Delta\mathbf{S}_{R,k}$.

A. Position error analysis

By the real robot path the parameter $\mathbf{B}_k$, $\Delta\mathbf{S}_{L,k}$ and $\Delta\mathbf{S}_{R,k}$ behavior are not linear, because they are affected with error. These errors cannot be solved by exact equation, however their state-space model can be considered as linear. With these errors can be separated in so called systematic and nonsystematic errors (Borenstein, 1997; Komoriya, 1994; Bostani, A., et al., 2008).

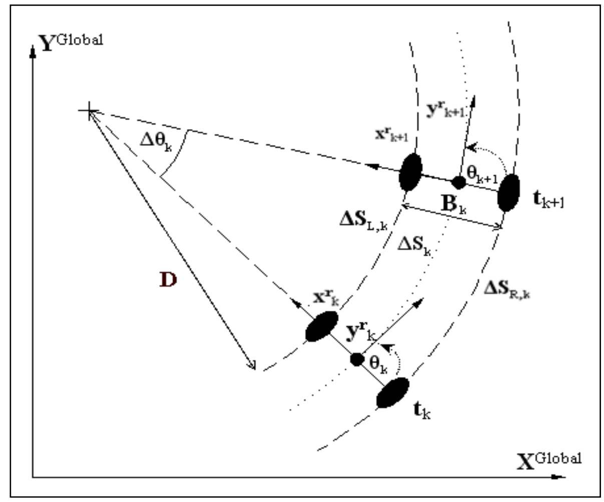

Fig.1. Kinematics relation between $\Delta\mathbf{S}_k$, $\Delta\boldsymbol{\theta}_k$, B_k, $\Delta\mathbf{S}_{L,k}$ and $\Delta\mathbf{S}_{R,k}$.

B. Wheel-base (distance between drive wheels) error

The wheel base is distance between both drive wheels. The distance B cannot be exactly measured because it can change during running (Bostani, A., et al., 2008). Uncertainty in the effective wheelbase is caused by the fact that rubber tires, which do not contact the floor in one point, but rather in a contact area. This resulting uncertainty about the effective wheelbase can be changed always during the robot run. This generates wheel-base error $\Delta\mathbf{B}_k$ and affects in equation (3) especially during fast turn. Therefore the rotation increment is affect by errors and the robot‘s orientation error is unbounded too.

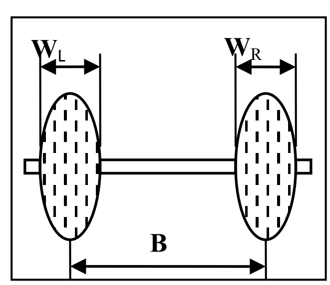

Fig.2.Wheel base of a mobile robot.

C. Theoretical wheel encoder model

The basic concept of odometry is the transformation from wheel revolution to linear translation on the floor (Naveen Kumar Boggarpu and Richard C. Kavanagh, 2010; Takeshi Sasaki, 2010). This transformation is affected with errors by wheel slippage, unequal wheel diameter, inaccurate wheel base distance, unknown factor and others. The real increment translation of wheel encoder is prone to systematic and some non-systematic errors. The theoretical translation and rotation increment at the center of the robot is calculated by

$$\Delta\mathbf{S}_{k}^{t}=\frac{\Delta\mathbf{S}_{R,k}^{t}+\Delta\mathbf{S}_{L,k}^{t}}{2}, \tag{2}$$

$$\Delta\boldsymbol{\theta}_{k}^{t}=\frac{\Delta\mathbf{S}_{R,k}^{t}-\Delta\mathbf{S}_{L,k}^{t}}{\mathbf{B}_{k}}. \tag{3}$$

Position extrapolation with theoretical encoder model is written as

$$\mathbf{P}_{k+1}^{t}=\mathbf{P}_{k}^{t}+\Delta\mathbf{P}_{k}^{t}, \tag{4}$$

and is detailed below

$$\mathbf{X}_{k+1}^{t}=\mathbf{X}_{k}^{t}+\Delta\mathbf{S}_{k}^{t}\cos\boldsymbol{\theta}_{k}^{t}, \tag{5}$$

$$\mathbf{Y}_{k+1}^{t}=\mathbf{Y}_{k}^{t}+\Delta\mathbf{S}_{k}^{t}\sin\boldsymbol{\theta}_{k}^{t}, \tag{6}$$

$$\boldsymbol{\theta}_{k+1}^{t}=\boldsymbol{\theta}_{k}^{t}+\Delta\boldsymbol{\theta}_{k}^{t}. \tag{7}$$

D. *Practical encoder model*

Incremental wheel encoders are based on the assumption that wheel revolutions can be translated into linear displacement relative to the floor. Wheel encoder error will occur, when if one wheel is to slip on, the associated encoder will not correctly correspond to a linear displacement of the wheel. All error sources are into one of two categories, which are systematic and non-systematic errors. Systematic errors are particularly considered, because they accumulate constantly, which can be reduced by careful mechanical design and by calibration. Non-systematic errors are not directly caused by the kinematic properties of the vehicle, example, wheel-slippage or irregularities of the floor. With smooth floor, systematic errors cause much more to wheel encoders errors than non-systematic errors. On rough surfaces non-systematic errors are the dominant source of wheel encoder errors. In practice encoders are prone to various systematic and non-systematic errors in the detection of $\Delta\mathbf{S}_{R,k}$ land $\Delta\mathbf{S}_{L,k}$. The output of ideal wheel encoder is corrupted by systematic error from hardware imperfections as time and temperature varying scale factor errors (Yang H., et al., 2000; Chung H., et al., 2001). From practical system inputs

$$\Delta\mathbf{S}_{R,k}^{p}=\left(1+\boldsymbol{\Omega}_{R,k}\right)g\Delta\mathbf{S}_{R,k}^{t}=\Delta\mathbf{S}_{R,k}^{t}+\boldsymbol{\Omega}_{R,k}\,g\Delta\mathbf{S}_{R,k}^{t}, \tag{8}$$

$$\Delta\mathbf{S}_{L,k}^{p}=\left(1+\boldsymbol{\Omega}_{L,k}\right)g\Delta\mathbf{S}_{L,k}^{t}=\Delta\mathbf{S}_{L,k}^{t}+\boldsymbol{\Omega}_{L,k}\,g\Delta\mathbf{S}_{L,k}^{t}, \tag{9}$$

and from equations (2), (3), (8) and (9) can be transformed in to a translation increment as

$$\begin{aligned}\Delta\mathbf{S}_{k}^{p}&=\frac{\Delta\mathbf{S}_{R,k}^{p}+\Delta\mathbf{S}_{L,k}^{p}}{2}\\&=\frac{(\Delta\mathbf{S}_{R,k}^{t}+\boldsymbol{\Omega}_{R,k}\,g\Delta\mathbf{S}_{R,k}^{t})+(\Delta\mathbf{S}_{L,k}^{t}+\boldsymbol{\Omega}_{L,k}\,g\Delta\mathbf{S}_{L,k}^{t})}{2}\end{aligned} \tag{10}$$

and rotation increment

$$\begin{aligned}\Delta\boldsymbol{\theta}_{k}^{p}&=\frac{\Delta\mathbf{S}_{R,k}^{p}-\Delta\mathbf{S}_{L,k}^{p}}{\mathbf{B}_{k}+\Delta\mathbf{B}_{k}}\\&=\frac{(\Delta\mathbf{S}_{R,k}^{t}+\boldsymbol{\Omega}_{R,k}\,g\Delta\mathbf{S}_{R,k}^{t})-(\Delta\mathbf{S}_{L,k}^{t}+\boldsymbol{\Omega}_{L,k}\,g\Delta\mathbf{S}_{L,k}^{t})}{\mathbf{B}_{k}+\Delta\mathbf{B}_{k}}\\&\quad Q\end{aligned}. \tag{11}$$

Position with practical encoder model can be estimated as

$$\begin{aligned}\mathbf{X}_{k+1}^{p}=\mathbf{X}_{k}^{p}&+\frac{(\Delta\mathbf{S}_{R,k}^{t}+\boldsymbol{\Omega}_{R,k}\,g\Delta\mathbf{S}_{R,k}^{t})\cos\boldsymbol{\theta}_{k}^{p}}{2}\\&+\frac{(\Delta\mathbf{S}_{L,k}^{t}+\boldsymbol{\Omega}_{L,k}\,g\Delta\mathbf{S}_{L,k}^{t})\cos\boldsymbol{\theta}_{k}^{p}}{2}\end{aligned} \tag{12}$$

$$\begin{aligned}\mathbf{Y}_{k+1}^{p}=\mathbf{Y}_{k}^{p}&+\frac{(\Delta\mathbf{S}_{R,k}^{t}+\boldsymbol{\Omega}_{R,k}\,g\Delta\mathbf{S}_{R,k}^{t})\sin\boldsymbol{\theta}_{k}^{p}}{2}\\&+\frac{(\Delta\mathbf{S}_{L,k}^{t}+\boldsymbol{\Omega}_{L,k}\,g\Delta\mathbf{S}_{L,k}^{t})\sin\boldsymbol{\theta}_{k}^{p}}{2}\end{aligned}, \tag{13}$$

$$\begin{aligned}\boldsymbol{\theta}_{k+1}^{p}=\boldsymbol{\theta}_{k}^{p}&+\frac{(\Delta\mathbf{S}_{R,k}^{t}+\boldsymbol{\Omega}_{R,k}\,g\Delta\mathbf{S}_{R,k}^{t})}{\mathbf{B}_{k}+\Delta\mathbf{B}_{k}}\\&-\frac{(\Delta\mathbf{S}_{L,k}^{t}+\boldsymbol{\Omega}_{L,k}\,g\Delta\mathbf{S}_{L,k}^{t})}{\mathbf{B}_{k}+\Delta\mathbf{B}_{k}}\end{aligned}. \tag{14}$$

Firstly, the error state $\boldsymbol{\delta}\mathbf{X}$ can be calculated by subtraction of the theoretical position values from practical position values yields the error propagation equations

$$\begin{aligned}\boldsymbol{\delta}\mathbf{X}_{k+1}=\boldsymbol{\delta}\mathbf{X}_{k}&+\frac{\boldsymbol{\Omega}_{R,k}\,g\Delta\mathbf{S}_{R,k}^{t}\cos\boldsymbol{\theta}_{k}^{t}}{2}+\frac{\boldsymbol{\Omega}_{L,k}\,g\Delta\mathbf{S}_{L,k}^{t}\cos\boldsymbol{\theta}_{k}^{t}}{2}\\&-\frac{(\Delta\mathbf{S}_{R,k}^{t}+\Delta\mathbf{S}_{L,k}^{t})\sin\boldsymbol{\theta}_{k}^{t}\,g\boldsymbol{\delta\theta}_{k}}{2}\end{aligned} \tag{15}$$

$$\begin{aligned}\boldsymbol{\delta}\mathbf{Y}_{k+1}=\boldsymbol{\delta}\mathbf{Y}_{k}&+\frac{\boldsymbol{\Omega}_{R,k}\,g\Delta\mathbf{S}_{R,k}^{t}\sin\boldsymbol{\theta}_{k}^{t}}{2}+\frac{\boldsymbol{\Omega}_{L,k}\,g\Delta\mathbf{S}_{L,k}^{t}\sin\boldsymbol{\theta}_{k}^{t}}{2}\\&+\frac{(\Delta\mathbf{S}_{R,k}^{t}+\Delta\mathbf{S}_{L,k}^{t})\cos\boldsymbol{\theta}_{k}^{t}\,g\boldsymbol{\delta\theta}_{k}}{2}\end{aligned} \tag{16}$$

$$\begin{aligned}\boldsymbol{\delta\theta}_{k+1}=\boldsymbol{\delta\theta}_{k}&+\frac{\boldsymbol{\Omega}_{R,k}\,g\Delta\mathbf{S}_{R,k}^{t}}{\mathbf{B}_{k}}-\frac{\boldsymbol{\Omega}_{L,k}\,g\Delta\mathbf{S}_{L,k}^{t}}{\mathbf{B}_{k}}\\&+\frac{(\Delta\mathbf{S}_{L,k}^{t}-\Delta\mathbf{S}_{R,k}^{t})g\Delta\mathbf{B}}{\mathbf{B}_{k}^{2}}\end{aligned}, \tag{17}$$

with the assumption that $\boldsymbol{\delta\theta}_{k}$ is small then $\cos\boldsymbol{\delta\theta}_{k}\approx 1$, $\sin\boldsymbol{\delta\theta}_{k}\approx\boldsymbol{\delta\theta}_{k}$, $\boldsymbol{\delta\theta}_{k}\,g\boldsymbol{\Omega}_{R,k}\approx 0$, $\boldsymbol{\delta\theta}_{k}\,g\boldsymbol{\Omega}_{L,k}\approx 0$ and $\mathbf{B}_{k}$? $\Delta\mathbf{B}_{k}$.

$$\begin{bmatrix} \delta\mathbf{X}_{k+1} \\ \delta\mathbf{Y}_{k+1} \\ \delta\boldsymbol{\theta}_{k+1} \\ \boldsymbol{\Omega}^{O}_{R,\,k+1} \\ \boldsymbol{\Omega}^{O}_{L,\,k+1} \\ \Delta\mathbf{B}_{k+1} \end{bmatrix} = \begin{bmatrix} 1 & 0 & -\frac{\Delta\mathbf{S}^{p}_{R,\,k}+\Delta\mathbf{S}^{p}_{L,\,k}}{2}\sin\boldsymbol{\theta}^{p}_{k} & \frac{\Delta\mathbf{S}^{t}_{R,\,k}\cos\boldsymbol{\theta}^{p}_{k}}{2} & \frac{\Delta\mathbf{S}^{t}_{R,\,k}\cos\boldsymbol{\theta}^{p}_{k}}{2} & 0 \\ 0 & 1 & \frac{\Delta\mathbf{S}^{p}_{R,\,k}+\Delta\mathbf{S}^{p}_{L,\,k}}{2}\cos\boldsymbol{\theta}^{p}_{k} & \frac{\Delta\mathbf{S}^{t}_{R,\,k}\sin\boldsymbol{\theta}^{p}_{k}}{2} & \frac{\Delta\mathbf{S}^{t}_{L,\,k}\sin\boldsymbol{\theta}^{p}_{k}}{2} & 0 \\ 0 & 0 & 1 & \frac{\Delta\mathbf{S}^{t}_{R,\,k}}{\mathbf{B}_{k}} & -\frac{\Delta\mathbf{S}^{t}_{L,\,k}}{\mathbf{B}_{k}} & -\frac{\Delta\mathbf{S}^{p}_{R,\,k}+\Delta\mathbf{S}^{p}_{L,\,k}}{\mathbf{B}^{2}_{k}} \\ 0 & 0 & 0 & 1 & 0 & 0 \\ 0 & 0 & 0 & 0 & 1 & 0 \\ 0 & 0 & 0 & 0 & 0 & 1 \end{bmatrix} \begin{bmatrix} \delta\mathbf{X}_{k} \\ \delta\mathbf{Y}_{k} \\ \delta\boldsymbol{\theta}_{k} \\ \boldsymbol{\Omega}^{O}_{R,\,k} \\ \boldsymbol{\Omega}^{O}_{L,\,k} \\ \Delta\mathbf{B}_{k} \end{bmatrix} \quad . (18)$$

Also the encoder scale factor of both wheels and wheel-base distance are regarded as random constants varying slightly in practice, so $\boldsymbol{\Omega}_{R/L,\,k+1} = \boldsymbol{\Omega}_{R/L,\,k}$, $\Delta\mathbf{B}_{k+1} = \Delta\mathbf{B}_{k}$.

E. *State space of navigation system*

A first-order linearization of equations (15)-(17) can be evaluated by Jacobians method and the result of navigation system matrix is detailed as equation (18). The state ariable, using $\mathbf{X}_k$ as the robot's position including some parameters of systematic errors is formulated as

$$\mathbf{x}^{O}_{k} = \begin{bmatrix} \mathbf{X}_{k} & \mathbf{Y}_{k} & \boldsymbol{\theta}_{k} & \boldsymbol{\Omega}^{O}_{R,\,k} & \boldsymbol{\Omega}^{O}_{L,\,k} & \Delta\mathbf{B}_{k} \end{bmatrix}^{T} . (19)$$

The position and heading is computed by the differential encoder. As the wheel diameter error (encoder scale factor error) and the wheel base error are the dominant systematic errors of the encoder, we are mainly concerned to reduce those errors using the gyroscope.

III. DIFFERENTIAL ODOMETRY INTEGRATED WITH GYROSCOPE

The creation of relative support for differential odometry is the compensation both translation and rotation increment. The relative support can compensate error from odometry system for translation and rotation increment. With compensation by relative support system can reduce errors generated by noise. This paper presents also relative support system of rotation increment $\Delta\boldsymbol{\theta}^{G}_{k}$ with gyroscope sensor. This work selects the commercial gyroscope CRS-03 (Silicon Sensing, 2000) working in measurement area ± 200°/s and $\Delta\theta^G = 3.2° \pm 0.01°$ shown in Fig.3.

A. *Gyroscope model*

Many researchers on robotic field work on about gyroscope sensor (Komoriya & Oyama, 1993; Karthick Srinivasan and Jason Gu, 2007). The theoretical gyroscope produces rotation increment in time interval k defined as $\Delta\boldsymbol{\theta}^{G,\,t}_{k}$. For position extrapolation with theoretical gyroscope is written as

$$\boldsymbol{\theta}^{G,\,t}_{k+1} = \boldsymbol{\theta}^{G,\,t}_{k} + \Delta\boldsymbol{\theta}^{G,\,t}_{k} . \qquad (20)$$

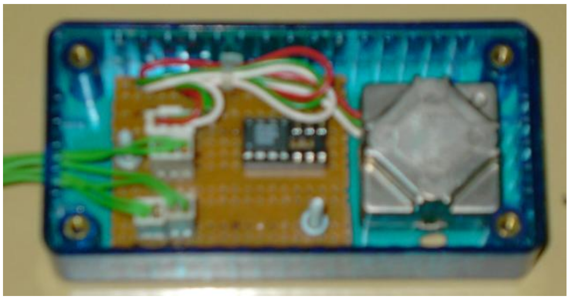

Fig.3.Gyroscope CRS03 with temperature compensation.

The practical gyroscope output

$$\Delta\boldsymbol{\theta}^{G,\,P}_{k} = \Delta\boldsymbol{\theta}^{G,\,t}_{k} + \boldsymbol{\Omega}^{G}_{k}\, g\Delta\boldsymbol{\theta}^{G,\,t}_{k} \qquad (21)$$

is corrupted by the scale factor error $\boldsymbol{\Omega}^{G}_{k}$ and bias $\boldsymbol{\Psi}^{G}_{k}$. The dominant gyroscope random errors are the random bias and the scale factor error. Generally, the gyroscope output signal is not zero even though there is no input and the effect of the earth rotation is neglected. The bias error of gyroscope is the signal output from the gyroscope when it is not any rotation. It is one of errors from gyroscope output reading. The bias error tends to vary with temperature and over time. The scale factor relates the output of the gyroscope to the corresponding gyroscope rotation angle about its input axis. By error of the scale factor in gyroscope it means the deviation between the actual scale factor and the nominal scale factor. The output beat frequency changes with the changing of the scale factor when the input rate is the same, which affects precision of gyro directly. For position extrapolation with practical gyroscope can be formulated as

$$\boldsymbol{\theta}^{G,\,p}_{k+1} = \boldsymbol{\theta}^{G,\,P}_{k} + \Delta\boldsymbol{\theta}^{G,\,P}_{k} = \boldsymbol{\theta}^{G,\,P}_{k} + \Delta\boldsymbol{\theta}^{G,\,t}_{k} + \boldsymbol{\Omega}^{G}_{k}\, g\Delta\boldsymbol{\theta}^{G,\,t}_{k} + \boldsymbol{\Psi}^{G}_{k} . \qquad (22)$$

The scale factor error $\boldsymbol{\Omega}^{G}_{k}$ and bias error $\boldsymbol{\Psi}^{G}_{k}$ can be regarded as random constants varying slightly in practical as $\boldsymbol{\Omega}^{G}_{k+1} = \boldsymbol{\Omega}^{G}_{k}$, $\boldsymbol{\Psi}^{G}_{k+1} = \boldsymbol{\Psi}^{G}_{k}$ .The error state vector is calculated by subtraction of the theoretical orientation value from practical orientation value yields the error orientation propagation

$$\delta\boldsymbol{\theta}^{G}_{k+1} = \delta\boldsymbol{\theta}^{G}_{k} + \boldsymbol{\Omega}^{G}_{k}\, g\Delta\boldsymbol{\theta}^{G,\,t}_{k} + \boldsymbol{\Psi}^{G}_{k} . \qquad (23)$$

$$\begin{bmatrix} \delta\mathbf{X}_{k+1} \\ \delta\mathbf{Y}_{k+1} \\ \delta\boldsymbol{\theta}_{k+1} \\ \boldsymbol{\Omega}^{O}_{R,k+1} \\ \boldsymbol{\Omega}^{O}_{L,k+1} \\ \Delta\mathbf{B}_{k+1} \\ \delta\boldsymbol{\theta}^{G}_{k+1} \\ \boldsymbol{\Omega}^{G}_{k+1} \\ \boldsymbol{\Psi}^{G}_{k+1} \end{bmatrix} = \begin{bmatrix} 1 & 0 & -\frac{\Delta\mathbf{S}^{p}_{R,k}+\Delta\mathbf{S}^{p}_{L,k}}{2}\sin\boldsymbol{\theta}^{p}_{k} & \frac{\Delta\mathbf{S}^{t}_{R,k}\cos\boldsymbol{\theta}^{p}_{k}}{2} & \frac{\Delta\mathbf{S}^{t}_{R,k}\cos\boldsymbol{\theta}^{p}_{k}}{2} & 0 & 0 & 0 & 0 \\ 0 & 1 & \frac{\Delta\mathbf{S}^{p}_{R,k}+\Delta\mathbf{S}^{p}_{L,k}}{2}\cos\boldsymbol{\theta}^{p}_{k} & \frac{\Delta\mathbf{S}^{t}_{R,k}\sin\boldsymbol{\theta}^{p}_{k}}{2} & \frac{\Delta\mathbf{S}^{t}_{L,k}\sin\boldsymbol{\theta}^{p}_{k}}{2} & 0 & 0 & 0 & 0 \\ 0 & 0 & 1 & \frac{\Delta\mathbf{S}^{t}_{R,k}}{\mathbf{B}_{k}} & -\frac{\Delta\mathbf{S}^{t}_{L,k}}{\mathbf{B}_{k}} & -\frac{\Delta\mathbf{S}^{p}_{R,k}+\Delta\mathbf{S}^{p}_{L,k}}{\mathbf{B}^{2}_{k}} & 0 & 0 & 0 \\ 0 & 0 & 0 & 1 & 0 & 0 & 0 & 0 & 0 \\ 0 & 0 & 0 & 0 & 1 & 0 & 0 & 0 & 0 \\ 0 & 0 & 0 & 0 & 0 & 1 & 0 & 0 & 0 \\ 0 & 0 & 0 & 0 & 0 & 0 & 1 & \Delta\boldsymbol{\theta}^{G,t}_{k} & 1 \\ 0 & 0 & 0 & 0 & 0 & 0 & 0 & 1 & 0 \\ 0 & 0 & 0 & 0 & 0 & 0 & 0 & 0 & 1 \end{bmatrix} \begin{bmatrix} \delta\mathbf{X}_{k} \\ \delta\mathbf{Y}_{k} \\ \delta\boldsymbol{\theta}_{k} \\ \boldsymbol{\Omega}^{O}_{R,k} \\ \boldsymbol{\Omega}^{O}_{L,k} \\ \Delta\mathbf{B}_{k} \\ \delta\boldsymbol{\theta}^{G}_{k} \\ \boldsymbol{\Omega}^{G}_{k} \\ \boldsymbol{\Psi}^{G}_{k} \end{bmatrix}$$

$$+\mathbf{w}_{k}\,. \tag{27}$$

$$\begin{aligned} \delta\mathbf{Z}^{OG}_{k} &= \delta\Delta\boldsymbol{\theta}^{O}_{k} - \delta\Delta\boldsymbol{\theta}^{G}_{k} \\ &= \left\{ \left[\frac{\boldsymbol{\Omega}_{R,k}\, g\Delta\mathbf{S}^{t}_{R,k}}{\mathbf{B}_{k}} \quad -\frac{\boldsymbol{\Omega}_{L,k}\, g\Delta\mathbf{S}^{t}_{L,k}}{\mathbf{B}_{k}} \quad \frac{(\Delta\mathbf{S}^{t}_{L,k}-\Delta\mathbf{S}^{t}_{R,k})g\Delta\mathbf{B}_{k}}{\mathbf{B}^{2}_{k}} \right] - \left[\boldsymbol{\Omega}^{G}_{k}\, g\Delta\boldsymbol{\theta}^{G,t}_{k} \quad \boldsymbol{\Psi}^{G}_{k} \right] \right\} + \mathbf{v}_{k} \end{aligned} \tag{28}$$

$$\delta\mathbf{Z}^{OG}_{k} = \begin{bmatrix} 0 & 0 & 0 & \frac{\Delta\mathbf{S}^{t}_{R,k}}{\mathbf{B}_{k}} & -\frac{\Delta\mathbf{S}^{t}_{L,k}}{\mathbf{B}_{k}} & \frac{\Delta\mathbf{S}^{t}_{L,k}-\Delta\mathbf{S}^{t}_{R,k}}{\mathbf{B}^{2}_{k}} & 0 & -\Delta\boldsymbol{\theta}^{G,t}_{k} & -1 \end{bmatrix} \begin{bmatrix} \delta\mathbf{X}_{k} \\ \delta\mathbf{Y}_{k} \\ \delta\boldsymbol{\theta}_{k} \\ \boldsymbol{\Omega}^{O}_{R,k} \\ \boldsymbol{\Omega}^{O}_{L,k} \\ \Delta\mathbf{B}_{k} \\ \delta\boldsymbol{\theta}^{G}_{k} \\ \boldsymbol{\Omega}^{G}_{k} \\ \boldsymbol{\Psi}^{G}_{k} \end{bmatrix} + \mathbf{v}_{k}\,. \tag{29}$$

B. State-space model of gyroscope

From a first-order linearization equation of gyroscope, the resulting time-variant perturbation model can be obtained by

$$\begin{bmatrix} \delta\boldsymbol{\theta}^{G}_{k+1} \\ \boldsymbol{\Omega}^{G}_{k+1} \\ \boldsymbol{\Psi}^{G}_{k+1} \end{bmatrix} = \begin{bmatrix} 1 & \Delta\boldsymbol{\theta}^{G,t}_{k} & 1 \\ 0 & 1 & 0 \\ 0 & 0 & 1 \end{bmatrix} \begin{bmatrix} \delta\boldsymbol{\theta}^{G}_{k} \\ \boldsymbol{\Omega}^{G}_{k} \\ \boldsymbol{\Psi}^{G}_{k} \end{bmatrix} + \mathbf{w}_{k}\,, \tag{24}$$

and

$$\delta\mathbf{X}^{G}_{k+1} = \mathbf{A}^{G}_{k}\delta\mathbf{X}^{G}_{k} + \mathbf{w}_{k}\,. \tag{25}$$

The state variable, using $\mathbf{x}^{G}_{k}$ including parameters of systematic error is obtained as $\mathbf{x}^{G}_{k} = \begin{bmatrix} \boldsymbol{\theta}^{G}_{k} & \boldsymbol{\Omega}^{G}_{k} & \boldsymbol{\Psi}^{G}_{k} \end{bmatrix}^{T}$.

C. Combination of state-space localization model between odometry and gyroscope

The combination of state space model can be written as

$$\delta\mathbf{X}^{OG}_{k+1} = \mathbf{A}^{OG}_{k}\delta\mathbf{X}^{OG}_{k} + \mathbf{w}_{k} \tag{26}$$

and detailed as equation (27).

D. Combination of odometry system and gyroscope by using different measurement model

The different measurement (Komoriya, 1994; Park, 1998) of rotation increment from the encoders and gyroscope is written as is calculated by equation (28) and detailed as equation(30). General form of different model between odometry system and gyroscope can be written as

$$\delta\mathbf{Z}^{OG}_{k} = \mathbf{H}^{OG}_{k}\delta\mathbf{X}^{OG}_{k} + \mathbf{v}_{k} \tag{30}$$

, where v_k is the measurement noise.

In this section, gyroscope is proposed to combine with odometry system for error compensation. The indirect Kalman filter which feeds back the error estimates to the main navigation algorithm mutually compensates the differential encoder errors and the gyroscope errors.

IV. ABSOLUTE POSITION SUPPORT WITH TRILATERATION ULTRASONIC POSITIONING SYSTEM (TUPS)

The design of navigation algorithm needs knowledge about ground truth. In order to quality of the estimated position $\widehat{\mathbf{P}}_{i} \approx \mathbf{P}^{Real}_{i}$ can be analyzed, $\mathbf{P}^{Real}_{i}$ must be known.

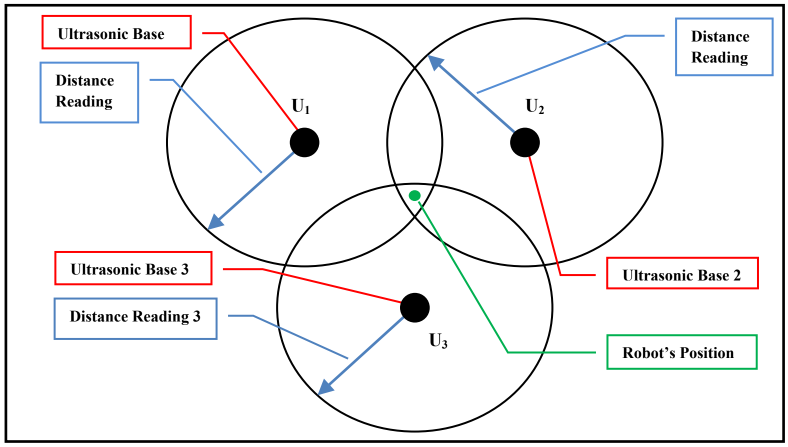

Fig.4 Principle geometry of robot's work space.

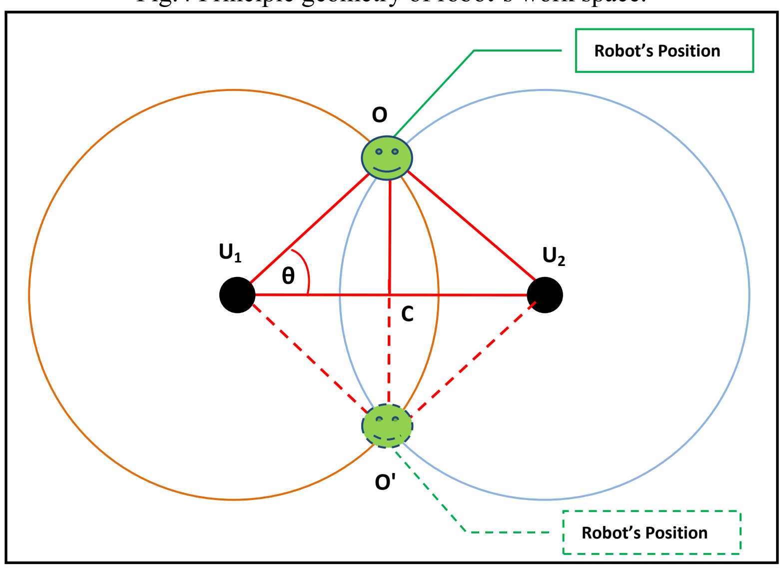

Fig.5 Intersection points from ultrasonic bases.

In practice on mobile robot field racks tool to measure $\mathbf{P}_i^{\text{Real}}$ and need more reference points to use $\mathbf{P}_i^{\text{Reference}}$ as $\mathbf{P}_i^{\text{Real}}$. The robot is stopped and its position is measured with measurement tape, but this method has disadvantages. The position error from position measurement with measurement tape can be not avoided. Because the robot must be stopped to mark a reference points, this damages the continuous dynamic of trajectory. This is the motivation to make a tool, which can support the absolute reference position ($\mathbf{P}_i^{\text{Reference}}$) for the mobile robot. The trilateration ultrasonic positioning system (**TUPS**) is designed for robot's positioning. It uses the principle of distance measurement that needs at least two landmarks with Cartesian's reference position. The principle geometry of robot's work space based on ultrasonic range is shown in Fig.4. The **TUPS** can calculate the object's position by using the relation of distance measurement from ultrasonic bases. With two ultrasonic distances from $\mathbf{U_1O}$ and $\mathbf{U_2O}$ and triangular relationship of $\triangle$ $\mathbf{U_1U_2O}$ from Pythagorean Theorem, the robot's position can be calculated and detailed later. From Fig.5 two ultrasonic send two intersection points, which are possible to be right (**O**) and false (**O'**) solution, so the third ultrasonic play an important role to specify the right solution. In work space limited in half area only two ultrasonic are required to determine the right solution. The first ultrasonic base is located at point $\mathbf{U_1}$ $(\mathbf{X_{u1}}, \mathbf{Y_{u1}})$ and another ultrasonic base is placed at point $\mathbf{U_2}$ $(\mathbf{X_{u2}}, \mathbf{Y_{u2}})$. Before the object's position can be calculated, it must be considered whether the intersection of two ultrasonic will occur or not. If the distance between point $\mathbf{U_1}$ and point $\mathbf{U_2}$ is more than the summation of distance reading from ultrasonic base 1 and 2, the intersection of two ultrasonic does not occur. Next, the robot's position (**O**) can be calculated from Pythagoras as below. From ultrasonic base 1, the relation is given as

$$(\mathbf{U_1C})^2 + (\mathbf{CO})^2 = (\mathbf{U_1O})^2, \tag{31}$$

and from ultrasonic base 2 is

$$(\mathbf{U_2C})^2 + (\mathbf{CO})^2 = (\mathbf{U_2O})^2. \tag{32}$$

From the subtraction of equation (1) and (2) the result is obtain as

$$(\mathbf{U_1C})^2-(\mathbf{U_2C})^2=(\mathbf{U_1O})^2-(\mathbf{U_2O})^2 \tag{33}$$

, then

$$[(\mathbf{U_1C})+(\mathbf{U_2C})][(\mathbf{U_1C})-(\mathbf{U_2C})]=(\mathbf{U_1O})^2-(\mathbf{U_2O})^2 \tag{34}$$

With $\mathbf{U_2C}=\mathbf{U_1U_2}-\mathbf{U_1C}$ and $\mathbf{U_1U_2}=\mathbf{U_1C}+\mathbf{U_2C}$, this gives the following expression as

$$[\mathbf{U_1C}-(\mathbf{U_1U_2}-\mathbf{U_1C})]*\mathbf{U_1U_2}=(\mathbf{U_1O})^2-(\mathbf{U_2O})^2, \tag{35}$$

and

$$2*\mathbf{U_1C}*\mathbf{U_1U_2}-(\mathbf{U_1U_2})^2=(\mathbf{U_1O})^2-(\mathbf{U_2O})^2, \tag{36}$$

then

$$\mathbf{U_1C}=\frac{(\mathbf{U_1O})^2-(\mathbf{U_2O})^2+(\mathbf{U_1U_2})^2}{2*\mathbf{U_1U_2}} \tag{37}$$

The angle (θ) is calculated as

$$\boldsymbol{cos\theta}=\frac{\mathbf{U_1C}}{\mathbf{U_1O}}, \tag{38}$$

and

$$\boldsymbol{\theta}=\boldsymbol{cos^{-1}}\left(\frac{\mathbf{U_1C}}{\mathbf{U_1O}}\right). \tag{39}$$

Finally, the robot's position is

$$\mathbf{X}^{\mathbf{ref.}}_{\mathbf{Robot}}=\mathbf{X}_{\mathbf{U_1}}+(\mathbf{U_1O})\boldsymbol{cos\theta}, \tag{40}$$

$$\mathbf{Y}^{\mathbf{ref.}}_{\mathbf{Robot}}=\mathbf{Y}_{\mathbf{U_1}}+(\mathbf{U_1O})\boldsymbol{sin\theta}. \tag{41}$$

In this section the **TUPS** as shown in figure 6 is in IKF-algorithm integrated. The absolute position of mobile robot is calculated from the **TUPS** and then fed to IKF algorithm. From equation (40) and (41) the absolute position (X^{Ref}, Y^{Ref}) of the robot can be generated from the **TUPS**. This absolute position from the **TUPS** will be compared with the absolute position from odometry integrated with gyroscope by using difference measurement of absolute position. The navigation method about absolute positioning system needs the environment map to localize the object's position.

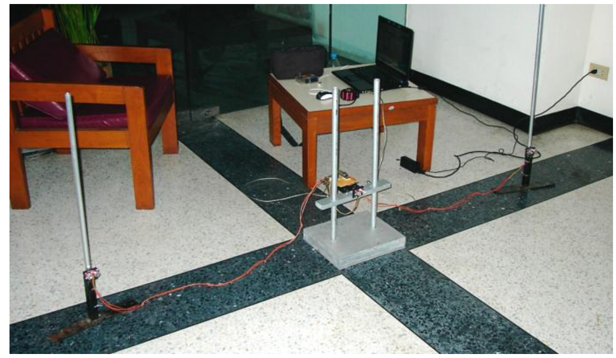

Fig.6.The **TUPS** Hardware.

In case of the **TUPS**, the navigation system of mobile robot does not need environment information, because the robot's absolute position is directly measured as

$$\mathbf{P}_k^{\mathrm{Ref}}=\begin{bmatrix}\mathbf{X}_k^{\mathrm{Ref}}\\ \mathbf{Y}_k^{\mathrm{Ref}}\end{bmatrix}=\mathbf{P}_k^{\mathrm{TUPS}}=\begin{bmatrix}\mathbf{X}_k^{\mathrm{TUPS}}\\ \mathbf{Y}_k^{\mathrm{TUPS}}\end{bmatrix}. \tag{42}$$

The TUPS can generate absolute position ($\mathbf{P}_k^{\mathrm{TUPS}}$) at center of mobile robot and the estimated position from odometry integrated with gyroscope can be calculated as

$$\hat{\mathbf{P}}_k^{\mathrm{OG}}=\begin{bmatrix}\hat{\mathbf{X}}_k^{\mathrm{OG}}\\ \hat{\mathbf{Y}}_k^{\mathrm{OG}}\end{bmatrix}. \tag{43}$$

By subtraction equation (43) from equation (42), a different measurement equation for position error is obtained by

$$\boldsymbol{\delta}\mathbf{P}_k^{\mathrm{OG,\,TUPS}}=\hat{\mathbf{P}}_k^{\mathrm{OG}}-\mathbf{P}_k^{\mathrm{TUPS}}=\begin{bmatrix}\hat{\mathbf{X}}_k^{\mathrm{OG}}\\ \hat{\mathbf{Y}}_k^{\mathrm{OG}}\end{bmatrix}-\begin{bmatrix}\mathbf{X}_k^{\mathrm{TUPS}}\\ \mathbf{Y}_k^{\mathrm{TUPS}}\end{bmatrix}. \tag{44}$$

V. HYBRID NAVIGATION SYSTEM FROM ABSOLUTE POSITIONING SYSTEM

This paper presents the systems of main differential odometry integrated with gyroscope in mobile robot.

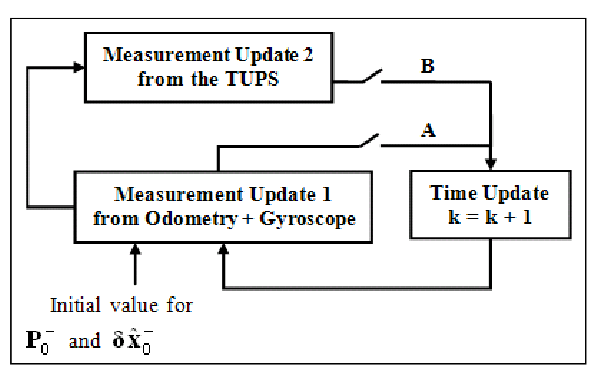

Fig.7.IKF loop the combination of support system and odometry system in measurement step.

Gyroscope generates rotation increment used to compensate rotation increment from differential odometry. The **TUPS** as the absolute positioning system is used as reference position for mobile robot. To construct the combination of the support system with odometry system of mobile robot is different measurement in the same physical variable, i.e. rotation or translation increment or absolute orientation or position between odometry and external support system. Then the estimate of error state $\delta\mathbf{X}$ from IKF (indirect Kalman filter) is calculated to correct the navigation state. The support systems are integrated in ―Measurement Update" step of IKF algorithm in Fig.7. If the connector **A** is only closed by software, the IKF loop to combine main odometry system and gyroscope is started. The IKF loop of odometry system integrated with gyroscope, which is combined with the **TUPS**, will start by only closed connector **B**.

A. The combination of odometry integrated with gyroscope and the TUPS

A state equation from basic odometry integrated with gyroscope is obtained by equation (27). The measurement equation $\mathbf{Z}_k = \mathbf{H}\mathbf{X}_k + \mathbf{V}_k$ between odometry integrated with gyroscope system and the **TUPS** can be written as

$$\mathbf{Z}_k = \hat{\mathbf{P}}_k^{OG} - \mathbf{P}_k^{TUPS} = \begin{bmatrix} \hat{\mathbf{X}}_k^{OG} \\ \hat{\mathbf{Y}}_k^{OG} \end{bmatrix} - \begin{bmatrix} \mathbf{X}_k^{TUPS} \\ \mathbf{Y}_k^{TUPS} \end{bmatrix} + \mathbf{v}_k . \quad (45)$$

Then the measurement matrix of equation (45) is

$$\mathbf{Z}_k^{OG,\,TUPS} = \begin{bmatrix} 1 & 0 & 0 & 0 & 0 & 0 & 0 & 0 & 0 \\ 0 & 1 & 0 & 0 & 0 & 0 & 0 & 0 & 0 \end{bmatrix} \begin{bmatrix} \delta\mathbf{X}_k \\ \delta\mathbf{Y}_k \\ \delta\boldsymbol{\theta}_k \\ \boldsymbol{\Omega}^{O}_{R,k} \\ \boldsymbol{\Omega}^{O}_{L,k} \\ \Delta\mathbf{B}_k \\ \delta\boldsymbol{\theta}^{G}_k \\ \boldsymbol{\Omega}^{G}_k \\ \boldsymbol{\Psi}^{G}_k \end{bmatrix} + \mathbf{v}_k$$

$$= \mathbf{H}_k^{OG,TUPS}\delta\mathbf{X}_k^{OG} + \mathbf{v}_k \quad (46)$$

, where $\mathbf{v}_k$ is the measurement noise.

B. Overall structure of navigation system

The main odometry integrated with gyroscope system and absolute positioning instruments (Byoung - Suk Choi, 2009; Luis M. Valentin-Coronado, et al., 2009) is shown in Fig.8. To estimate the absolute orientation error, the different orientation between compass and odometry system integrated with gyroscope is used as a measurement value in IKF loop. In IKF loop error parameters of main system are also estimated and fed back to correct encoder error and gyroscope error.

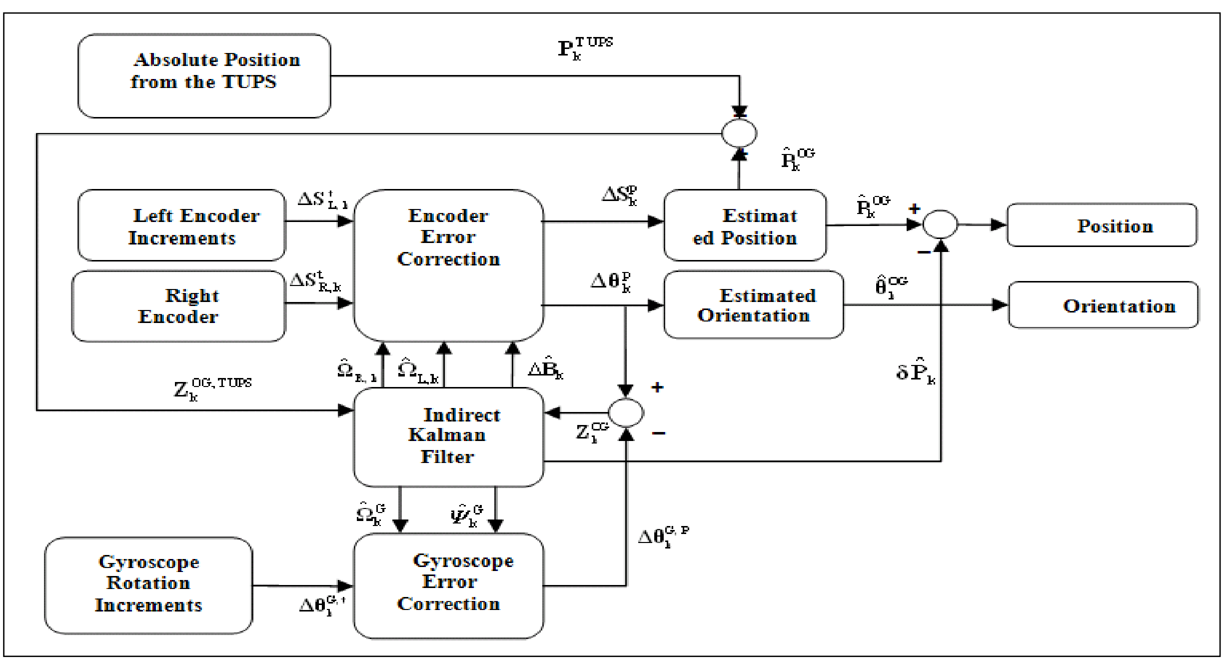

Fig.8.Overall combinations of support system and odometry system.

VI. SIMULATION AND EXPERIMENTAL RESULTS

The navigation error state from odometry $\delta\mathbf{X}^{O}$ occurring during long trajectory and high dynamic environment is reduced by linear state vector and estimated by IKF algorithm. To keep the position estimation of mobile robot with pinpoint accuracy is based on the reciprocal error compensation between odometry error and gyroscope error.

A. Result of combination with gyroscope support

The mobile robot (Pioneer-II from active media company) driven by differential odometry system integrated with gyroscope and compass shown in Fig.7 is used for experiment in square shape 2.5x2.0 m. In experiment the robot starts at the position coordinate (x = 0, y = 0, θ = 0˚) and runs from start point in right direction and returns at the start point again with speed 0.2 m/s.

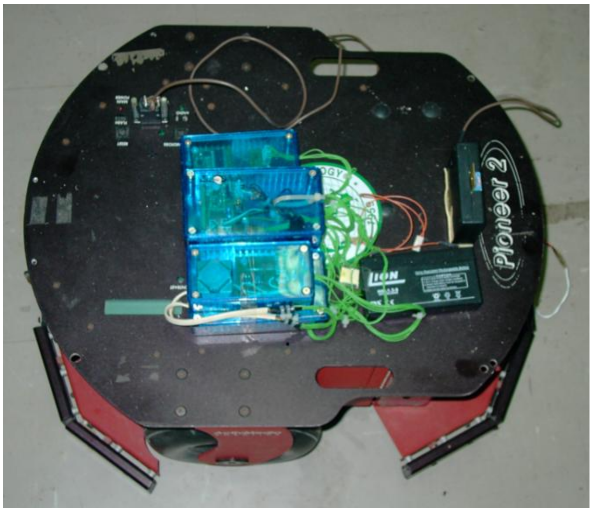

Fig.9.Pioneer-II integrated with gyroscope.

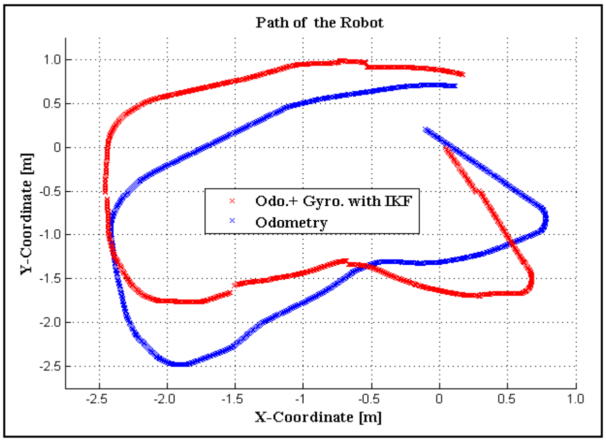

Fig.10 Position generated by encoders is shown in blue line and the red line shows the position estimation of the robot by using different measurement of rotation increment between encoders and gyroscope with IKF algorithm.

From experiment the robot's final position from odometry system are $\hat{\mathbf{P}}^{O}$ ($\hat{x}^{O} = 18.4$ cm , $\hat{y}^{O} = 71.1$ cm) and from odometry system integrated with gyroscope $\hat{\mathbf{P}}^{OG}$ ($\hat{x}^{OG} = 20.7$ cm , $\hat{y}^{OG} = 85.4$ cm) as shown in Fig.10. Also systematic errors of odometry system are shown in Fig.11 and gyroscope in Fig.12 and detail in Table 1.

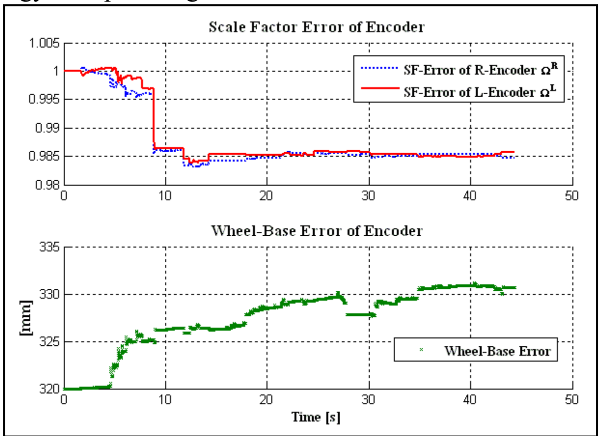

Fig.11.Systematic error of odometry system.

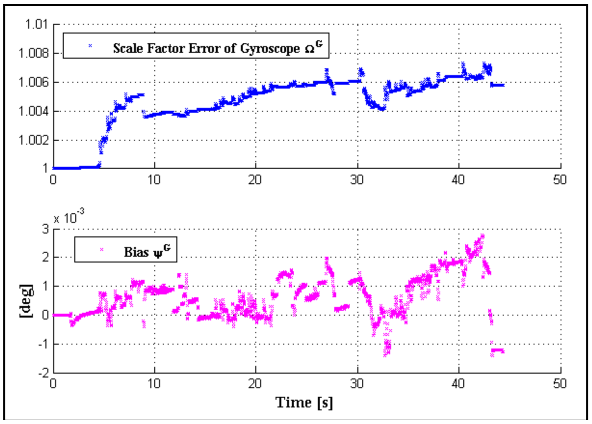

Fig.12.Systematic error of gyroscope.

For the navigation algorithm the reference position plays an important role. To reduce position error of odometry, the reference position must be known to find the difference position between odometry system and reference position in time.

B. Result of combination with the TUPS support

In this section, details the powerful IKF algorithm with the TUPS support. The TUPS concept is more details in previous section. In Fig.13 shows the graphic of robot's trajectory in square shape from the TUPS compared with the reference point. The different measurement of position $\hat{\mathbf{P}}^{OG,IKF}$ and $\mathbf{P}^{TUPS}$ as shown in Fig.14 will be send to the second measurement update as shown in Fig.7 to reduce absolute position error. In Fig.15 shows trajectory of the robot running from the calculated position $\mathbf{P}^{O}$ from odometry equation, $\mathbf{P}^{TUPS}$ generated by the TUPS and estimated position $\hat{\mathbf{P}}$ with gyroscope and the TUPS support by using IKF algorithm. For the navigation algorithm the reference position plays an important role. To reduce position error of odometry, the reference position must be known to find the difference position between odometry system and reference position in time. Generally the reference positions are constructed by manual measurement, which is difficult and not possible to measure the reference position in time. But the TUPS can generate the reference or absolute position compared with position from odometry system in the same time. In Table 2 shows the results of final coordinate of robot trajectory compared with actual reference coordinate.

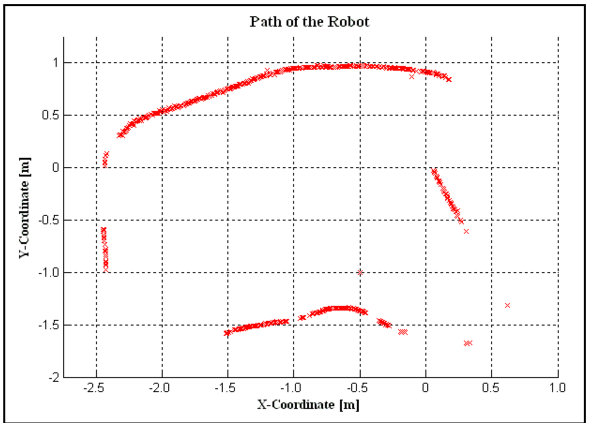

Fig.13.Absolute position generated by the TUPS compared with the reference position.

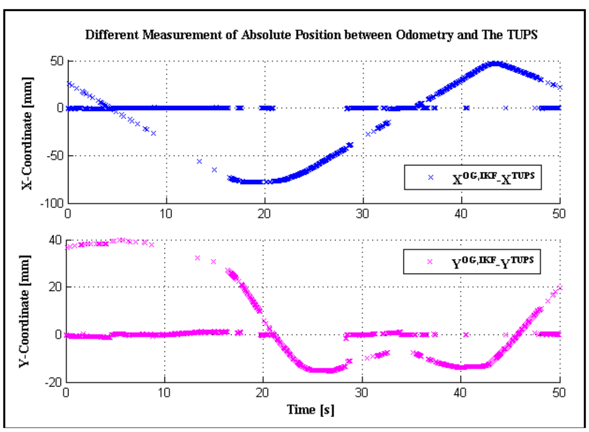

Fig.14.Difference absolute positions between estimate positions from odometry integrated with gyroscope and from the TUPS.

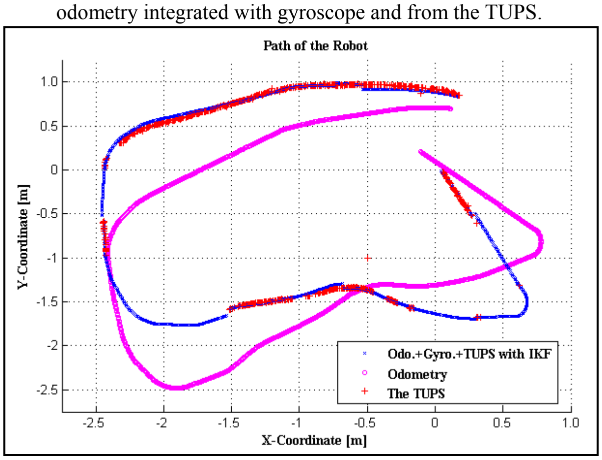

Fig.15.Implement of the TUPS positioning system in IKF algorithm for estimate of robot position in global coordinate.

VII. CONCLUSION

This paper proposed the hybrid absolute positioning system using trilateration ultrasonic positioning system for odometry system integrated with gyroscope for mobile robot in an indoor environment. To reduce the absolute position error, the TUPS is combined with odometry system integrated with gyroscope. The indirect feedback Kalman filter (IKF) is used as the combination of odometry system, gyroscope and the absolute orientation to estimate and compensate errors. The IKF can estimate the error of estimated absolute position by using the information from the TUPS. Then mobile robot's position and orientation are obtained from addition of the estimated position and orientation error with the estimated position and orientation from main system. Also the IKF estimated the scale factor error of encoders, the distance error between wheels and scale factor and bias errors of gyroscope to correct errors from encoders and gyroscope. The simulation results show that the IKF can give precisely estimated position and orientation by using absolute positioning system. Further research aims to support the translation increment for odometry system with an accelerometer. The complementary measurement between translation increment from encoder and accelerometer can be passed to the filter.

REFERENCES

1. **Shoichi Maeyama, Nobuyuki Ishikawa and Shin'ichi Yuta**. **1996**. Rule based filtering and fusion of odometry and gyroscope for a fail safe dead reckoning system of a mobile robot, IEEE International Conference on Multi sensor Fusion and Integration for Intelligence Systems, pp.541-548.
2. **Y. Watanabe and S. Yuta. 1990.** Position Estimation of Mobile Robots with Internal and External Sensors Using Uncertainty Evolution Technique, Proceedings of IEEE International Conference on Robotics and Automation Vol.3, pp.2011-2016.
3. **Shoichi Maeyama, Akihisa Ohya and Shin'ichi Yuta**. **1995**. Non-stop outdoor navigation of a mobile robot - Retroactive positioning data fusion with a time consuming sensor system, IEEE/RSJ International Conference on Intelligent Robot and Systems, vol.1, pp.130-135.
4. **S. Maeyama, A. Ohya and S. Yuta. 1994**. Positioning by tree detection sensor and dead- reckoning for outdoor navigation of a mobile robot, IEEE International Conference on Multi sensor Fusion and Integration Systems, pp. 653-660.
5. **J. Borenstein and L. Feng. Gyrodometry**. **1996**. A new method for combining data from gyroscope and odometry in Mobile Robots, IEEE International

Conference on Robotics and Automation, Vol.1,pp.423-428.

6. **J. Borenstein, H.R.Everett, L.Feng, and D. Wehe. 1997**. Mobile Robot Positioning-Sensor and Techniques, Journal of Robotic System, Vol. 14, No.4, pp.231-249.
7. **Hakyoung Chung, Lauro Ojeda and Johann Borenstein**. **2001**. Sensor Fusion for Mobile Robot Dead-Reckoning with A Precision-Calibrated Fiber Optic Gyroscope, IEEE, Seoul, Korea, May 21-26, pp.3588-3593.
8. **Borenstein J. and Feng L. 1997**. Measurement and correction of Systematic Odometry Errors in Mobile Robots, IEEE Trans. On Robotic and Automation, Vol.12, No.6, pp.869-880, 1640-1648.
9. **K. Komoriya and E. Oyama**. **1994**. Position Estimation of a Mobile Robot Using Optical Fiber Gyroscope (OFG, Proc. IROS'94, pages 143-149,
10. **Britting, K.R**. **1971**. Inertial Navigation Systems Analysis, Wiley Interscience, Newyork, USA.
11. **Kelly, A. 2001**. A General Solution for Linearized Systematic Error Propagation in Vehicle Odometry, in Proceedings of the 2001 JEEE/RSJ International Conference on Intelligent Robots and Systems, Band 4, 5. 1938-1945.
12. **Larsen, T. D., Bak, M., Aurlersen, N, A. & Ravn, O**. **1998**. Location Estimation for an Autonomously Guided Vehicle Using an Augmented Kalman Filter to Auto calibrate the odometry in Proceedings of the 1st international Conference on Multisource - Multisensor Information Fusion, Band 1, S. 21-27.
13. **Chnug. H, O.jeda, L. & Borenstein, J**. **2001**. Accurate Mobile Robot Dead-Reckoning with a Precision-calibrated Fiber-optic Gyroscope, IEEE Transactions on Robotics and Automation 17. S. 80-84.
14. **Mayback, P.S. 1979**. Stochastic Models, Estimation and Control, Band 141 in Mathematics in Science and Engineering, Academic Press, New York, USA.
15. **Barshan, B., and Durrant-Whyte, H. F. 1995**. Inertial Navigation Systems for Mobile Robots. IEEE Transaction on Robotics and Automation, vol.11, June, pp. 328-342.
16. **Park, K., Chung, H., and Lee, J. 199l.** Dead Reckoning Navigation for Autonomous Mobile Robots. Proc .of Intelligent Autonomous Vehicle, Madrid, Spain, March 25-28, pp. 775-781.
17. **Kakuba and Arenas. 1987.** Position Verification of a Mobile Robot Using Standard Pattern" IEEE Journal of Robotics and Automation, vol. RA-3, NO.6, December, pp.505-516.
18. **Sony Corporation, 2004**. Color Digital Camera DFW-SX910 Technical Manual.
19. **Ojeda, L. and Borenstein, J. 2000.** Experimental Results with the KVH C-100 Fluxgate Compass in Mobile Robots. Proceedings of the IASTED International Conference Robotics and Applications 2000 August 14-16, Honolulu, Hawaii, USA, pp.1-7.
20. **Brown, R. 1997.** Introduction to random signals and applied Kalman filtering with Matlab exercises and solutions third edition, ISBN: 978-0-471-12839-7, Wiley, New York.
21. **Xie, M. 2003.** Fundamentals of robotics linking perception to action, ISBN: 981-238-313-1, World Scientific Publishing Co. Pte. Ltd., Singapore.
22. **Panich, S. 2008.** A Mobile Robot with a Inter–Integrated Circuit System. IEEE 10th International Conference on Control, Automation, Robotics & Vision, December 17-20, Hanoi, Vietnam, pp. 2010-2014.
23. **Naveen Kumar Boggarpu and Richard C. Kavanagh. 2010.** New Learning Algorithm f or High-Quality Velocity Measurement and Control When Using Low-Cost Optical Encoders, IEEE Transactions on Instrumentation and Measurement, vol. 59, no. 3, March, pp. 565-574.
24. **Ali Bostani, Ahmad Vakili and Tayb.A.Denidni. 2008.** A Novel Method to Measure and Correct the Odometry Errors in Mobile Robots, 21th Canadian Conference on Electrical and Computer Engineering (CCECE), May 5-7, Ontario, Canada, pp.897-900.
25. **Byoung-Suk Choi. 2009.** Mobile Robot Localization in Indoor Environment using RFID and Sonar Fusion System, IEEE/RSJ International Conference on Intelligent Robots and Systems October 11-15, St. Louis, USA, pp. 2039-2044.
26. **Srinivasan, K. and Gu, J. 2007.** Multiple Sensor Fusion in Mobile Robot Localization, 20th Canadian Conference on Electrical and Computer Engineering (CCECE), April 22-26, Vancouver British Columbia, Canada, pp.1207-1210.
27. **Diansheng Chen, Feng Bai and Lin Wu**. **2008.** Kinematics Control of Wheeled Robot Based on

Angular Rate Sensors, IEEE Conference on Robotics, Automation and Mechatronics, September 21-24, Chengdu, China, pp. 598-602.

28. **Takeshi Sasaki. 2010**. Human-Observation-Based Extraction of Path Patterns for Mobile Robot Navigation, IEEE Transactions on Industrial Electronics, vol. 57, no. 4, pp.1401 - 1410.
29. **Luis M. Valentin-Coronado, Victor Ayala-Ramirez and Raul E. Sanchez-Yanez**, 2009. Error Modeling of Mapping Approaches Using Mobile Robots, University of Guanajuato IEEE Students Chapter (IEEExPO),
30. **Sotirios Ch. Diamantas and Richard M. Crowder**. **2009**. Localization and Mapping Using a Laser Range Finder: A Goal-Seeking Approach. Fifth International Conference on Autonomic and Autonomous Systems, April 20- 25, Valencia, Spain, pp.270-276.
31. **Kang Li, Han-Shue Tan, and J. Karl Hedrick. 2009**. Map-Aided GPS/INS Localization Using a Low-Order Constrained Unscented Kalman Filter. Joint 48th IEEE Conference on Decision and Control and 28th Chinese Control Conference Shanghai, P.R. China, December 16-18, pp.4607-4612.